Available online at www.sciencedirect.com
SCIENCE DIRECT®
Planetary and Space Science 52 (2004) 1023–1037
Planetary and Space Science
www.elsevier.com/locate/pss

Detectability of minor constituents in the martian atmosphere by infrared and submillimeter spectroscopy

Th. Encrenaz[a,*], E. Lellouch[a], S.K. Atreya[b], A.S. Wong[b]

[a]*LESIA, Observatoire de Paris, 92195 Meudon, France*
[b]*Department of Atmospheric, University of Michigan, Oceanic, and Space Sciences, Ann Arbor, MI 48109-2143, USA*

Available online 25 August 2004

Abstract

Spectroscopic remote sensing in the infrared and (sub)millimeter range is a powerful technique that is well suited for detecting minor species in planetary atmospheres (Planet Space Sci. 43(1995) 1485). Yet, only a handful of molecules in the Mars atmosphere (CO_2, CO and H_2O along with their isotopic species, O_3, and more recently H_2O_2 and CH_4) have been detected so far by this method. New high performance spectroscopic instruments will become available in the future in the infrared and (sub)millimeter range, for observations from the ground (infrared spectrometers on 8 m class telescopes, large millimeter and submillimeter interferometers) and from space, in particular the Planetary Fourier Spectrometer (PFS) aboard Mars Express (MEx), and the Heterodyne Instrument for the Far-Infrared (HIFI) aboard the Herschel Space Observatory (HSO). In this paper we will present results of a study that determines detectability of minor species in the atmosphere of Mars, taking into account the expected performance of the above spectroscopic instruments. In the near future, a new determination of the D/H value is expected with the PFS, especially during times of maximum H_2O abundance in the martian atmosphere. PFS is also expected to place constraints on the abundance of several minor species (H_2O_2, CH_4, CH_2O, SO_2, H_2S, OCS, HCl) above any local outgassing sources, the hot spots. It will be possible to obtain complementary information on some minor species (O_3, H_2O_2, CH_4) from ground-based infrared spectrometers on large telescopes. In the more distant future, HIFI will be ideally suited for measuring the isotopic ratios with unprecedented accuracy. Moreover, it should be able to observe O_2, which has not yet been detected spectroscopically in the IR/submm range, as well as H_2O_2. HIFI should also provide upper limits for several species that have not yet been detected (HCl, NH_3, PH_3) in the atmosphere of Mars. Some species (SO, SO_2, H_2S, OCS, CH_2O) that may be observable from the ground could be searched for with present single-dish antennae and arrays, and in the future with the Atacama Large Millimeter Array (ALMA) submillimeter interferometer.

Keywords: Mars; Mars atmosphere; Infrared spectroscopy; Submillimeter spectroscopy

Abbreviation: ALMA, Atacama large millimeter array; CRIRES, Cryogenic IR echelle spectrometer; CSO, Caltech submillimeter observatory; ESO, European southern observatory; GEISA, Gestion et Etude des Informations Spectroscopiques Atmosphériques; HIFI, Heterodyne instrument for the far-infrared; HSO, Herschel space observatory; IRAM, Institut de Radio Astronomie Millimétrique; IRIS, Infrared interferometer spectrometer; IRTF, Infrared telescope facility; ISM, Infrared spectrometer; ISO, Infrared space observatory; LWS, Long wavelength spectrometer; SWS, Short wavelength spectrometer; JCMT, James clerk maxwell telescope; MAWD, Mars atmospheric water detection; Mex, Mass express; MGS, Mars global surveyor; MIRO, Microwave instrument for the rosetta orbiter; NEB, Noise equivalent brightness; OVRO, Owens valley radio observatory; PFS, Planetary fourier spectrometer; SWAS, Submillimeter wave astronomical satellite; TES, Thermal emission spectrometer; TEXES, Texas Echelon Cross Echelle spectrograph; VIRTIS, Visible infrared thermal imaging spectrometer; VIRTIS-H, VIRTIS-high resolution channel; VLT, Very large telescope.

*Corresponding author. Tel.: +33-1-4507-7691; fax: +33-1-4507-2806.
E-mail address: therese.encrenaz@obspm.fr (T. Encrenaz).

0032-0633/$ - see front matter © 2004 Elsevier Ltd. All rights reserved.
doi:10.1016/j.pss.2004.07.011

1. Introduction

The infrared/(sub)millimeter range is especially suited for searching for spectral signatures of minor molecular species of the martian atmosphere. This is because the maximum of the thermal emission occurs in the mid-infrared around 20 μm, where molecules exhibit their strongest signatures due to rotation lines or fundamental vibration–rotation bands.

However, infrared and millimeter spectra of Mars have so far exhibited few spectral signatures of minor atmospheric species. CO_2, CO, H_2 and their isotopes, ozone O_3, and recently H_2O_2 and CH_4, are the only species that have been detected spectroscopically in the infrared. Space observations were achieved by the Infrared Interferometer Spectrometer (IRIS) on Mariner 9, the Viking Mars Atmospheric Water Detectors (MAWD), the Short Wavelength Spectrometer (SWS) and the Long Wavelength Spectrometer (LWS) on the Infrared Space Observatory (ISO). Ground-based observations at high spectral resolution were obtained in the near-infrared range (including first detection of HDO; Owen et al., 1988), in the mid-infrared range (detection of O_3, Espenak et al., 1991) and in the millimeter range (first detection of CO, Kakar et al., 1977; detection of H_2O, Clancy et al., 1992, Novak et al., 2002; detection of HDO and H_2 ^{18}O, Encrenaz et al., 1991, 2001a; Clancy et al., 1996). The spatial distribution of CO was also studied from ground-based near-infrared spectroscopy (Krasnopolsky et al., 2003). Upper limits of several minor species have been obtained from the IRIS-Mariner data (Maguire, 1977), the ISO-SWS (Lellouch et al., 2000), and ground-based millimeter measurements (Encrenaz et al., 1991). H_2O_2, which had been unsuccessfully searched for (Krasnopolsky et al., 1997; Encrenaz et al., 2002) has been detected from ground-based high-resolution spectroscopic measurements in the submillimeter range (Clancy et al., 2004) and around 8 μm (Encrenaz et al., 2003, 2004) during the 2003 opposition of Mars. Finally, the tentative detection of CH_4 has been also recently reported from ground-based near-IR high-resolution spectroscopy (Mumma et al., 2003; Krasnopolsky et al., 2004) and from PFS/Mex (Formisano et al., 2004a).The composition of the lower martian atmosphere, as currently known, is shown in Table 1a, and current upper limits of the various atmospheric constituents are summarized in Table 1b.

The present work is an update and an extension toward infrared wavelengths of a study that was done for the detectability of minor species in planetary atmospheres in the millimeter and submillimeter range (Encrenaz et al., 1995). In this paper, we make quantitative estimates of detectability limits of minor species in the martian atmosphere, using presently envisioned future space and ground-based spectroscopic capabilities. These future space instruments are the infrared Planetary Fourier Spectrometer aboard Mars Express (PFS, 2–45 μm, $\Delta\nu = 2\,cm^{-1}$), and the HIFI heterodyne spectrometer aboard Herschel Space Observatory (HIFI, 16–64 cm^{-1}, $R = 10^6$). We also note the IR channel of the SPICAM instrument aboard Mars Express (1.1–1.8 μm, $R = 1500$). Infrared ground-based high-resolution spectroscopy can also be performed in some atmospheric windows, in particular in the near-infrared range (J, H, K, L filters), around 5 μm (M filter) and at 7–13 μm (N filter). Examples of existing instruments are, at the Infrared Telescope Facility (IRTF) of the Mauna Kea Observatory, the imaging spectrometer SpeX in the 2–5 μm range ($R = 2000$) and TEXES

Table 1a
Composition of the lower martian atmosphere

Gaseous species	Abundance (mixing ratio)
CO_2	95.32%
N_2	2.7%
^{40}Ar	1.6%
O_2	0.13%
CO	0.07%
H_2O	10–1000 ppm (variable)
$^{36+38}Ar$	5.3 ppm
Ne	2.5 ppm
Kr	0.3 ppm
Xe	0.08 ppm
O_3	0.04–0.2 ppm (variable)
H_2O_2	20–40 ppb (variable)
CH_4	10 ppb

Updated from Owen (1992) and Encrenaz (2001).

Table 1b
Upper limits of minor species in the martian atmosphere

Species	Upper limit (mixing ratio)	Type of observation	Reference
C_2H_2	2×10^{-9}	IRIS-Mariner 9	Maguire (1977)
C_2H_4	5×10^{-7}	IRIS-Mariner 9	Maguire (1977)
C_2H_6	4×10^{-7}	IRIS-Mariner 9,	Maguire (1977)
C_2H	4×10^{-7}	IRIS-Mariner 9	Maguire (1977)
N_2O	1×10^{-7}	IRIS-Mariner 9	Maguire (1977)
NO_2	1×10^{-8}	IRIS-Mariner 9	Maguire (1977)
NH_3	5×10^{-9}	IRIS-Mariner 9	Maguire (1977)
PH_3	1×10^{-7}	IRIS-Mariner 9	Maguire (1977)
SO_2	3×10^{-8}	Ground-based,mm	Encrenaz et al. (1991)
OCS	7×10^{-8}	Ground-based,mm	Encrenaz et al. (1991)
H_2S	2×10^{-8}	Ground-based,IR	Encrenaz et al. (1991)
CH_2O	3×10^{-9}	Ground-based,IR	Krasnopolsky et al. (1997)
HCl	2×10^{-9}	Ground-based,IR	Krasnopolsky et al. (1997)

Updated from Maguire (1997) and Encrenaz (2001).

Table 2
Observational means

Instrument	Space/ground-based	Spectral range (cm^{-1})	Spectral range (GHz)	Resolving power	Spatial resolution on Mars (km)
PFS/Mex	Space (Mars orbit)	220–8000	—	$\Delta\nu = 2\,cm^{-1}$	5–10
VIRTIS-H/Rosetta	Space (Mars flyby)	2000–5000	—	2000	
MIRO/Rosetta	Space (Mars flyby)	18.5	557	10^6	
HIFI/Herschel	Space (Earth orbit)	16–64	480–1920	10^6	Integrated disk
CRIRES/VLT	Ground-based	2000–10000	—	10^5	200 (0.5 arcs)
TEXES/IRTF	Ground-based	700–1400	—	10^5	200 (0.5 arcs)
ALMA	Ground-based	3–24	86–720	10^6	80 (0.2 arcs)

(Texas Echelon Cross Echelle Spectrograph) at 7–13 μm ($R = 10^5$). In the future, as an example, the Cryogenic IR Echelle Spectrometer (CRIRES) instrument at the Very Large Telescope (VLT) of European Southern Observatory (ESO), will combine, in the 1–5 μm range, very high sensitivity and high resolving power ($R = 10^5$). In the millimeter range, heterodyne spectroscopy ($R = 10^6$), especially at Owens Valley Radio Observatory (OVRO) and Institut de Radio Astronomie Millimétrique (IRAM), have given information on H_2O, CO and temperature vs. pressure in the martian atmosphere. In the submillimeter range, antennas of 10–15 m in diameter are currently available at the James Clerk Maxwell Telescope (JCMT) and at the Caltech Submillimeter Observatory (CSO). In the future, the ground-based millimeter/submillimeter interferometer ALMA, with 64 antennas of 12 m diameter, will combine an unprecedented sensitivity, a high spectral resolving power ($R = 10^6$) and a high spatial resolution (<0.2 arcs), up to a frequency of about 1 THz. Two IR/submm instruments aboard the Rosetta spacecraft, launched in March 2004, will observe Mars during its flyby of the planet en route to the mission target, comet Churyumov–Gerasimenko. The Visible Infrared Thermal Imaging Spectrometer (VIRTIS) on Rosetta is an infrared imaging spectrometer with a high-resolution channel (VIRTIS-H) operating between 2 and 5 μm with a resolving power of 2000, whereas Microwave Instrument for the Rosetta Orbiter (MIRO) is a heterodyne spectroscopy receiver which will observe atmospheric species in a few selected channels around the 557 GHz transition of water vapor (Encrenaz et al., 2001b). Table 2 shows a summary of the spectroscopic techniques, along with their expected performance, that are included in the present study.

The PFS has a limited spectral resolution, but its high spatial resolving power will make it the best tool available for investigating locally enhanced species. The ground-based infrared spectrometer CRIRES will offer a very good combination of both high spatial and spectral resolution in all infrared windows observable from the ground. We note that HIFI will be well suited for placing stringent upper limits on very low abundance species. Since in most cases, the diffraction limit of the instrument exceeds the size of the martian disk even at high frequency, the HIFI observations will integrate over the whole disk.

2. Selection of molecular species

The lower atmosphere of Mars (Table 1a) is composed of CO_2 (95.32% per volume), N_2 (2.7%), ^{40}Ar (1.6%), O_2 (0.13%), CO (0.07%), and H_2O (seasonally variable, from 10 to 1000 ppm). As mentioned above, CO_2, CO, H_2O, with their isotopes, H_2O_2 and possibly CH_4 have been detected by IR spectroscopy, while O_2 was detected from visible spectroscopy (Carleton and Traub, 1972). N_2, ^{40}Ar, O_2 and O_3 abundances were measured by Viking mass spectroscopy (Nier and McElroy, 1977; Owen et al., 1977). In the middle atmosphere (50–70 km), O_3 has been detected spectroscopically in the UV (Barth et al., 1973) and in the IR range (Espenak et al., 1991), but the derived abundances were very different. Barth et al. (1973) reported abundances as high as 40 μm am in the vicinity of the pole, while only 2 μm am were measured by Espenak et al. (1991). The latter suggested the possibility of a local enhancement, or possible adsorption of O_3 on the ice. NO has been detected in the thermosphere in situ from Viking mass spectrometry observations (Nier and McElroy, 1977).

Apart from these detected species, we consider two classes of possible candidate minor species: (1) products expected from photochemistry models, and (2) products expected from possible local outgassing. For completeness we also consider three other photochemical products, HO_2, an important intermediate radical in the martian photochemistry, and two other nitrous species, NO_2 and N_2O.

Any localized hot spot on Mars could also be a source of H_2O, CO_2, SO_2, H_2S, possibly CH_4 and, to a lesser extent, halogens. CH_4 was tentatively identified in trace amounts, and the sulfur species have not been detected so far in the atmosphere of Mars. However, their flux into the atmosphere could result in photochemical production of several new species, including SO, SO_3, OCS, CH_2O, CH_3OH, C_2H_6 and HCl, amongst others

Table 3
Molecular species considered in the present study

(uma) species	IR wavenumber (cm^{-1})	Log line intensity (GEISA)	Sub-mm frequency (GHz)	Log line intensity (JPL)
(16)CH_4	3032	−3.0	—	—
(17)NH_3	949	−1.9	1215	−0.6
(18)H_2O	3854	−0.3	1163	−0.3
(19)HDO	2721	−1.2	1217	−0.6
(19)$H_2^{17}O$	—	—	1149	−0.3
(20)$H_2^{18}O$	—	—	1137	−0.3
(28) CO	2147	−0.6	1152	−2.4
(29)^{13}CO	2100	−0.6	1211	−2.4
(29)$C^{17}O$	2120	−0.6	1235	−2.4
(30)$C^{18}O$	2096	−0.6	1207	−2.4
(30)CH_2O	2822	−0.7	674[b]	−1.0
(30)NO	—	—	1153	−3.1
(32)O_2	—	—	1121	−5.8
(33)HO_2	—	—	1120	−1.9
(34)H_2S	1293[a]	−2.3	611[b]	−1.9
(34)H_2O_2	1234	−1.3	1160	−1.3
(34)PH_3	1122[a]	−1.4	1067	−1.7
(35) HCl	2776	−0.05	1251	−0.4
(44)CS	—	—	685[b]	−0.5
(48)O_3	1055	−0.9	1180	−2.6
(48)SO	—	—	688[b]	−1.2
(60)OCS	2071	0.3	474[b]	−2.2
(64)SO_2	1361	−0.9	689[b]	−2.3

Note: Log I is the intensity parameter as defined in the JPL data base and pertains to a rotational temperature of 300 K. It is related to the line strength S through $I = 3 \times 10^{18}$ S [in cm^{-1} $(mol\ cm^{-2})^{-1}$ at 300 K.
The S parameter is listed in the GEISA database.
[a]From Maguire (1977).
[b]From Encrenaz et al., 1995.

(Wong et al., 2003). Most of these species are calculated to have less than 1 ppb mixing ratios. NH_3 and PH_3 may also be outgassed, but their abundances are not expected to be significant; we nevertheless include them in our list for completion, as these species are abundant in the tropospheres of the giant planets.

For estimating limits of possible detections of hot spots with PFS, we need to use relatively short integration times. In the vicinity of the pericenter, the distance observed by Mars Express at the surface of Mars, in the nadir mode, is about 30 km in ten seconds (typical measurement cycle duration of PFS), and 200 km in 1 min. These numbers are comparable to the sizes of the calderas of the larger volcanoes, and are smaller than the width of Valles Marineris. We consider them as suitable for estimating the detectability of localized phenomena.

Table 3 lists all molecules considered in this work, along with the frequencies and strengths of their most favorable (i.e. intense) transitions (or examples of them, when many lines of same intensities occur), in the IR (220–8000 cm^{-1}) and the submillimeter (16–64 cm^{-1}) range. It is important to point out two things about the entries in this Table. First, as the Martian atmosphere is very tenuous with a mean surface pressure less than 10 mbar, the lines have a typical Lorentz half-width of about 20 MHz (0.0006 cm^{-1}), so they are separated in almost all cases at infinite resolution. As a result, in the infrared range, the intensities of individual transitions are better indicators than integrated band strengths of vibration–rotation bands. Second, in the case of the submillimeter range, we have taken into account the sensitivity of the detectors which provides an important constraint. Indeed, in the case of HIFI/Herschel, the best sensitivity is achieved in the 1100–1260 GHz range (37–42 cm^{-1}) while it is degraded by a factor of ~ 5 in the 1400–1800 GHz range (47–60cm^{-1}). We have thus selected the strongest lines of the 1100–1260 GHz range, even when slightly stronger transitions appear at higher frequency. In the case of PFS, we also take into account the variation of the NEB (noise equivalent brightness) as a function of the wavelength.

3. Radiative transfer modeling

We have used a standard atmospheric profile of the martian atmosphere corresponding to mean seasonal

and latitudinal conditions, with a mean surface pressure of 7.5 mbar, and a mean surface temperature of 250 K, an atmospheric temperature of 225 K at the surface and 175 K at an altitude of 20 km. The mean surface emissivity is assumed to be 0.9, corresponding to a dielectric constant of 2.5. Above 50 km, the thermal profile is isothermal at 150 K. These average conditions are consistent with the results obtained from the space missions Mariner 9, Viking and Mars Global Surveyor (MGS) (see, in particular, Martin and Kieffer, 1979; Santee and Crisp, 1993; Smith et al., 2001). Note however, the surface temperature on the martian disk is very inhomogeneous, with local maxima possibly as high as 300 K; in such case, the thermal infrared flux coming from the whole disk is strongly weighted toward this hot region. In addition, if the surface temperature is significantly higher (i.e. by more than 10 K) than the atmospheric temperature in the boundary layer at the surface, as is frequently observed, the observed depth of a weak line may be significantly enhanced. As a result, the detectability limits derived in the present study are expected to be conservative and should be considered only as estimates, as they strongly depend upon the atmospheric parameters used in the calculations.

Below a wavelength of 4.5–5 μm, the contribution of the reflected solar component must be taken into account. For typical martian conditions (surface albedo of 0.3, surface temperature of 250 K), the solar component becomes dominant below the strong CO_2 absorption at 4.25 μm. An example of the integrated spectrum of Mars, showing the contribution of both reflected and thermal components, is shown by the ISO data (see Fig. 2 of Lellouch et al., 2000). Below 4.5 μm, we consider both components, with the relative weights corresponding to the ISO data. Calculations show that the reflected component is favorable for searching minor species because, for a given line intensity, the depth of the line is stronger in the reflected regime than in the thermal one. Also, we note that this depth is much less sensitive to atmospheric parameters than in the thermal regime. Only the continuum level is affected, to first order, by the surface albedo; the line depth is insensitive to the albedo in a non-scattering regime, and is affected only in the case of a strong dust opacity.

Spectroscopic parameters were taken from the Gestion et Etude des Informations Spectroscopiques Atmosphériques (GEISA) data bank (Jacquinet-Husson et al., 1999; http://ara.lmd.polytechnique.fr/alexei_index.html) for the infrared range, and from the Poynter-Pickett Catalog (http://spec.jpl.nasa.gov) for the submillimeter range.

The radiative transfer code is described in Lellouch et al. (1989, 1991) and in Encrenaz et al. (1995). An air mass of 1.6 was assumed for calculations corresponding to disk-resolved observations. It corresponds to intermediate spectra between limb and nadir in the case of PFS observations and VIRTIS-H/MIRO observations at the time of the Rosetta flyby. We also performed calculations for the integrated-disk case, for comparison with the HIHI measurements. Note that these two types of calculation may be significantly different, as the limb contribution is not taken into account in the first case. If there is a weak contrast between the surface and atmospheric temperatures, the limb contribution, in the calculation of very weak lines, tends to build emission wings around the central core, as the atmospheric temperature at low altitudes is larger than the surface emission because the surface emissivity is lower than 1. This effect is illustrated, in particular, in the synthetic spectra shown by Encrenaz et al. (1995) and Lellouch et al. (2000). As mentioned above, the present results can only be considered as first-order estimates, as, in the thermal range, the synthetic spectra of very weak lines depend crucially upon the adequate atmospheric and surface parameters. Specific calculations, corresponding to the exact observing conditions, will have to be performed on a case-by-case basis in order to interpret all observations in the thermal regime.

4. Results

4.1. Water vapor (H_2O) and its isotopes

Water vapor dominates both the infrared and the submillimeter spectrum of Mars. In the 220–8000 cm^{-1} range (PFS), H_2O can be best detected in three regions (Lellouch et al., 2000): the 2.6 μm range (ν_1 and ν_3 bands, in the blue wing of a strong ν_4 CO_2 absorption band), at 6.2 μm (ν_2 band), and in the rotational band at 20–45 μm. A weaker band, used by the MAWD Viking instrument, also appears at 1.38 μm, and can be observed by PFS and SPICAM aboard Mars Express. The H_2O rotational band also dominates the entire submillimeter range; one of the strongest H_2O transitions, at 557 GHz, was detected on Mars with the SWAS submillimeter satellite (Gurwell et al., 2000), and later with the ODIN satellite (Biver et al., 2004).

Observations of H_2O on Mars using IRIS-Mariner 9, MAWD-Viking and the Thermal Emission Spectrometer (TES) on MGS have provided us with precise maps of the water vapor content and its seasonal and latitudinal variations (see for instance Jakosky and Haberle, 1992; Smith, 2002). With a column abundance ranging between 1 and 80 pr μm (corresponding to mean mixing ratios of approximately 10^{-5} to 10^{-3}), water vapor will be detectable with PFS under most circumstances. The ISO spectrum (Lellouch et al., 2000) corresponds to a mean H_2O abundance of 15 pr μm($\sim$ 150 ppm). We note that for such an abundance and greater values, condensation of water vapor

takes place in the martian atmosphere, as shown also by Clancy et al. (1996) from millimeter observations. Therefore the column density of H_2O and its mean mixing ratio are not exactly proportional. In the case of the ISO observations (July 31, 1997, $L_s = 157^\circ$), for an abundance of 15 pr μm, the condensation level was found to be at about 10 km (Lellouch et al., 2000).

In addition to the measurement of H_2O itself (e.g. with PFS or HIFI), it is particularly interesting and important to study its isotopic species using PFS. The HDO/H_2O ratio, in particular, is a key parameter for understanding the history of water and the climate on Mars. In the case of the oxygen isotopes, determining the isotopic ratios at the percent level of accuracy in H_2O, and comparing the corresponding values in CO_2 and CO, will help us understand better the history of various volatile reservoirs (Owen, 1992). Previous ground-based measurements of HDO have indicated a deuterium enrichment of about 6 ± 3 (Owen et al., 1988) and 5.5 ± 2 (Krasnopolsky et al., 1997) relative to the terrestrial value. In both observations, the large uncertainty comes from the difficulty of determining precisely HDO and H_2O simultaneously, because of the large amount of water in the Earth's atmosphere. Space observations are thus best suited for this study.

In the case of PFS, the ISO spectra provide a good analogue, as ISO has a spectral resolution comparable to the PFS in the 2.3–5 μm range ($\Delta\nu = 2\,cm^{-1}$ at 2.4 μm). As shown in Fig. 7 of Lellouch et al. (2000), the presence of HDO is best observed around 3.675 μm as a change of the continuum between solar lines. For $H_2O = 15$ pr μm, the change is 1%. We can thus expect to detect HDO with the PFS when the water abundance is at its maximum (when the areocentric longitude L_s is about 100–120°), with a contrast of a few percent. A typical value of the continuum level is $0.3\,erg/s/cm^2sr/cm^{-1}$ at 3.7 μm. The expected NEB of PFS is $0.05\,erg/s/cm^2sr/cm^{-1}$. According to the H_2O seasonal distribution monitored by MGS (Smith, 2002), the region where H_2O is above 50 pr μm extends over northern latitudes of 60N–80N, which corresponds to a distance of about 1000 km at the martian surface, observed by Mars Express in about 5 min, if the spacecraft is in the vicinity of the pericenter. In 5 min of integration time, we can expect a S/N of about 80 on the continuum, which should translate into a S/N of about 3 in the HDO contrast (4%) when the water vapor abundance is maximum (above 50 pr μm). As the area of maximum water vapor extends over longitudes, observations from several consecutive orbits can be added. By adding data from about 10 orbits at the proper latitude, we can hope to reach a S/N of 10. Note that this S/N could be improved if observations at higher airmass are performed. The present accuracy of the D/H ratio in the atmosphere of Mars should thus be improved by the PFS data.

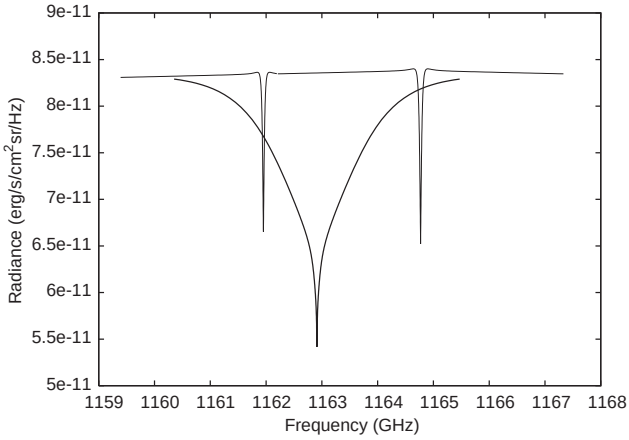

Fig. 1. The disk-integrated synthetic spectrum of H_2O on Mars calculated in the 1159–1168 GHz range under nominal conditions (see text), showing the strong H_2O transition at 1163 GHz (bold line) and two weaker HDO transitions at 1162 and 1165 GHz (thin line). The H_2O mean mixing ratio is 1.5×10^{-4} (15 pr μm), and the D/H ratio is 6 times the terrestrial value. Calculations are relevant to HIFI observations. The spectral resolution is 1 MHz ($R = 10^6$).

Subsequently, the use of HIFI in the submillimeter range should improve the martian D/H measurement by another order of magnitude. Fig. 1 shows the disk-integrated synthetic spectrum of a strong H_2O transition and two weaker HDO lines around 1163 GHz. The most favorable transitions of HDO occur at 1162, 1165 and 1217 GHz. The line contrast, for the mean H_2O abundance of 15 pr μm (mean mixing ratio of 1.5×10^{-4}) is about 30%. In this frequency range, the estimated time needed to measure the martian continuum with a S/N of 100 is about 70 s. We can thus expect, assuming no contamination by ripples, a S/N above 200 in the strongest HDO line (1217 GHz) in only one hour of integration time. In the same way, oxygen isotopes of water vapor will be best measured at 1136 GHz ($H_2^{18}O$) and 1149 GHz ($H_2^{17}O$), with expected S/N of 500 and 100, respectively, in 1 h of integration time . In conclusion, HIFI appears to be the best tool for measuring isotopic ratios from water on Mars.

4.2. Carbon monoxide (CO) and its isotopes

CO is detectable on Mars through its two vibrational bands, (1-0) at 4.7 μm and (2-0) at 2.35 μm. Both the (1-0) and the (2-0) bands should be easily observable with PFS. Previous IR spectra of CO were obtained from the ground (Billebaud et al., 1992, 1998), by ISO at 4.7 μm (see Fig. 2 of Lellouch et al., 2000) and by the Infrared Spectrometer ISM on the Phobos spacecraft at 2.35 μm (Rosenqvist et al., 1992). The ground-based study of the CO (3-0) band at 1.6 μm has shown evidence for a north–south asymmetry of the CO abundance (Krasnopolsky et al., 2003). The main interest in studying CO with the PFS lies in the monitoring of this

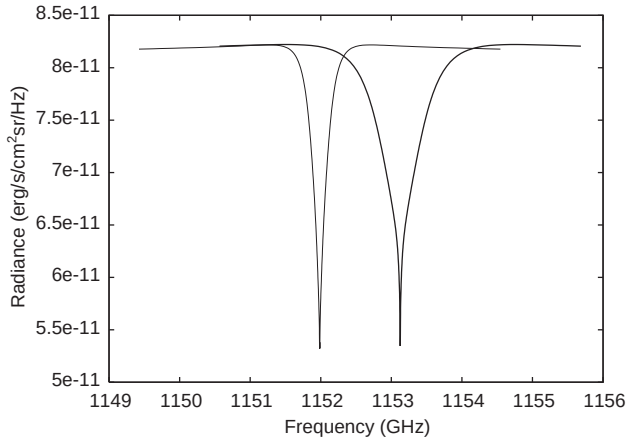

Fig. 2. The disk-integrated synthetic spectrum of H_2O and CO on Mars calculated in the 1149–1156 GHz range under nominal conditions (see text), showing the strong H_2O transition at 1153 GHz (bold line) and the (10-9) CO transition at 1152 GHz (thin line). The H_2O mean mixing ratio is 1.5×10^{-4} (15 pr μm), and the CO mixing ratio is 7×10^{-4}. Calculations are relevant to HIFI observations. The spectral resolution is 1 MHz ($R = 10^6$).

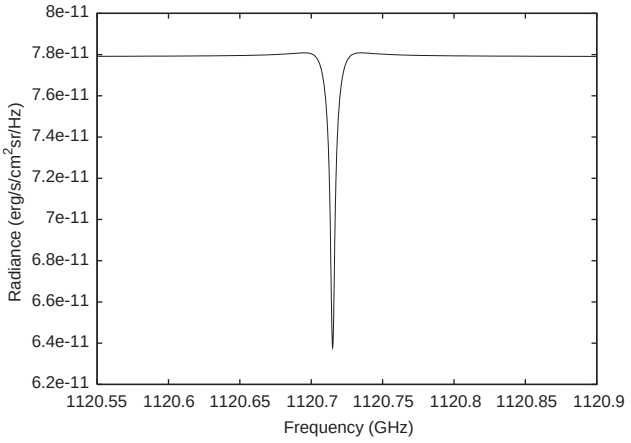

Fig. 3. Synthetic spectrum of the oxygen transition at 1120.67 GHz, calculated for the integrated disk, as a simulation of HIFI observations The oxygen mixing ratio is 0.0013. The spectral resolution is 1 MHz ($R = 10^6$).

effect, and also in the search for possible local variations of this species, as an unexpected behavior was apparently observed along the flanks of the Tharsis volcanoes with the ISM (Rosenqvist et al., 1992) and more recently with the PFS (Formisano et al., 2004b).

CO on Mars has been studied extensively from the ground using its millimeter rotational transitions (1-0, 2-1 and 3-2 at 115, 230 and 345 GHz, respectively). Observations of CO and ^{13}CO have been used to determine the CO abundance over the planet and to constrain the martian thermal structure (Clancy et al., 1990, 1996). CO has also been mapped over the martian disk to retrieve the wind velocity field (Lellouch et al., 1991). This program should greatly benefit in the future from the high spatial resolution of the ALMA array.

^{13}CO and $C^{18}O$ should be also detectable with HIFI, but other transitions of lower J-values are also observable from the ground using large single dish antennas, and a better sensitivity is expected in the future with ALMA. Fig. 2 shows the CO (10-9) transition with a strong H_2O neighboring line as will be seen by HIFI.

4.3. Oxygen (O_2)

The oxygen abundance in the martian atmosphere was measured by ground-based high-resolution spectroscopy in the visible range (Carleton and Traub, 1972). It was later confirmed by the Viking mass spectrometers, giving a mixing ratio of 0.0013 (Owen et al., 1977).

The oxygen molecule, with no permanent dipole moment, has only weak spectroscopic signatures through its quadrupole transitions. For the 1121 GHz transition, our calculations predict a depth of about 15% (Fig. 3), which should be easily detected with HIFI. The oxygen measurement may seem to be of limited interest, as oxygen is expected to be uniformly distributed over the planet due to its long photochemical lifetime, but possibility of surprises due to dynamical or other effects may not be ruled out.

4.4. Ozone (O_3)

As mentioned above, ozone was detected on Mars using two different means which led to very different estimates of the ozone abundance: UV spectroscopy from space (Barth et al., 1973) and IR ground-based high-resolution spectroscopy (Espenak et al., 1991; Novak et al., 2002). Photochemical models predict strong seasonal variations over the martian disk, with a local maximum in O_3 at an altitude of about 50 km (Krasnopolsky, 1993; Atreya and Gu, 1994; Nair et al., 1994). They also predict that the O_3 and H_2O abundances should be anticorrelated because of the loss of O_3 on HO_x. The SPICAM instrument aboard Mars Express will be best suited for measuring the O_3 vertical distribution with its UV stellar occultation mode, and, using its near-IR channel, to study its anticorrelation with the H_2O abundance.

We now consider the detectability of ozone in the IR range. Fig. 4 shows a calculation of the O_3 spectrum of Mars in the 1046–1064 cm^{-1} region, which includes the strongest absorption lines of the O_3 vibration–rotation band centered at 9.5 μm. The assumed column density of 2.5×10^{17} cm^{-2}, corresponding to a mean vertical mixing ratio of 10^{-6}. This value is significantly higher than the IR measurements (4×10^{15} cm^{-2}), and also

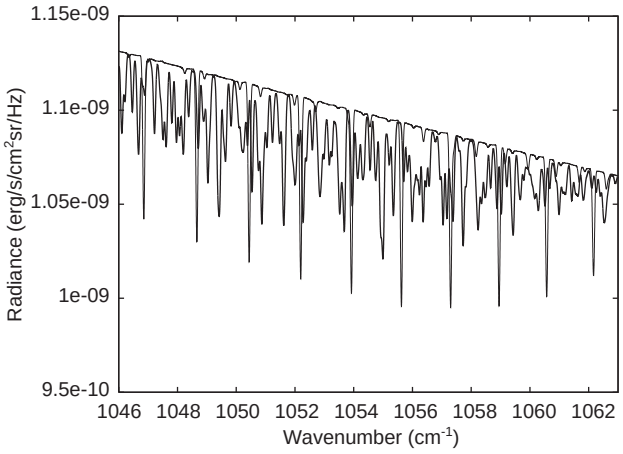

Fig. 4. Synthetic spectrum of ozone between 1046 and 1064 cm^{-1}, calculated with an airmass of 1.6. The ozone mean mixing ratio is $10^{-6}(2 \times 10^{18}\,cm^{-2})$. The spectral resolution is 0.1 cm^{-1}. Bold line: O_3 lines; thin line: CO_2 isotopic lines.

larger than the UV results (about $10^{17}\,cm^{-2}$). Such an abundance thus represents an upper limit of what could ever be expected on Mars, even in the presence of a local maximum of ozone. Calculations performed at a spectral resolution of 0.1 cm^{-1}, corresponding to a resolving power of 10^4, indicate a mean depth of 7%. If such an instrument was available in Earth orbit or around Mars, ozone would be easily detectable, even probably with an abundance ten times lower. Presently, only moderate spectral resolution is available with PFS. At 2 cm^{-1} resolution, all O_3 signatures disappear and the band is no more detectable. In addition, the O_3 band appears in a region where the surface of Mars exhibits distinct signatures due to silicates, which would make the identification even more difficult at moderate resolution. In summary, besides the SPICAM observations in the UV range, the best method for monitoring O_3 on Mars in the IR is presently to use high-resolution ground-based spectroscopy in the 10 μm region, as was done by Espenak et al. (1991) and Novak et al. (2002), and to take advantage of a maximum Doppler shift to separate the martian lines from the telluric ones as much as possible.

In the submillimeter range, ozone transitions would be easily detectable in the 1100–1260 GHz range, assuming the same high mean mixing ratio of 10^{-6}. In particular, with HIFI, the 1180.3 GHz transition would show a depth of 14% (Fig. 5a). Another band also appears around 1214 GHz with about the same intensity (Fig. 5b), and should be also a good indicator of the ozone abundance. Assuming an O_3 column density of 4 $10^{15}\,cm^{-2}$, as derived from IR observations, the expected line depth of the O_3 lines, as seen by HIFI, should be 0.2%. In 4 h of integration time, ozone could then be detectable at the 3-σ level.

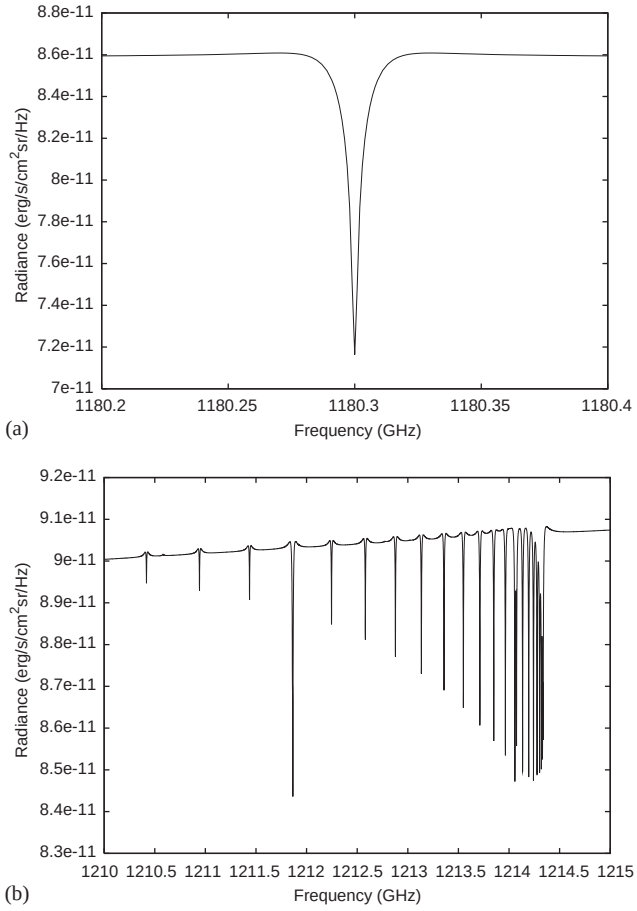

Fig. 5. (a) Synthetic spectrum of the ozone transition at 1180.3 GHz, calculated for the integrated disk (HIFI simulation). The ozone mean mixing ratio is $10^{-6}(2.5 \times 10^{17}\,cm^{-2})$. The spectral resolution is 1 MHz ($R = 10^6$). (b) Synthetic spectrum of the ozone absorption band between 1210 and 1215 GHz, calculated for the integrated disk. The ozone mean mixing ratio is $10^{-6}(2.5 \times 10^{17}\,cm^{-2})$. The spectral resolution is 1 MHz ($R = 10^6$).

4.5. Hydrogen peroxide (H_2O_2)

H_2O_2 could be the elusive oxidant on Mars, and could explain the lack of organics on this planet. This explanation was proposed, in particular, as an interpretation of the results of the biology experiments on the Viking landers (Klein et al., 1992). Photochemical models predict H_2O_2 to be correlated with the H_2O abundance, with a mean mixing ratio as high as 10^{-8} (Krasnopolsky, 1993; Atreya and Gu, 1994; Nair et al., 1994). H_2O_2 has been detected in 2003 from ground-based high-resolution spectroscopy (Clancy et al., 2004; Encrenaz et al., 2004), with a mixing ratio of 2–4 $\times 10^{-8}$ (corresponding to a column density of 4–8 $\times 10^{16}\,cm^{-2}$). However, the upper limit of $10^{15}\,cm^{-2}$ obtained in 2001 by Encrenaz et al. (2002), for a different value of the areocentric longitude L_s, shows evidence for strong seasonal variations.

The best spectral range for searching for H_2O_2 is 1225–1245 cm^{-1}(8.1 μm). As shown by Encrenaz et al.

(2002; Fig. 3 of their paper), for a mean mixing ratio of 10^{-7}, the mean depth of the lines, with a spectral resolution of 0.017 cm^{-1}, is 1.7%. PFS, with its 2 cm^{-1} moderate spatial resolution, will thus be unable to detect H_2O_2. We note, in addition, that a strong torsion-rotation band of H_2O_2 is present around 30 μm (Perrin et al., 1996). However, the absolute positions and intensities of the individual lines are not published or available so far (Perrin and Flaud, 2003, private communication). Unfortunately, the PFS spectral resolving power at 30 μm is only about 200 or less, which puts a severe limitation on the detection capabilities of this instrument in the far-infrared range. As in the case of ozone, ground-based high-resolution spectroscopy at 8 μm is expected to be the most sensitive technique for mapping H_2O_2 on Mars.

H_2O_2 also shows transitions in the submillimeter range. Many lines, stronger than the 364 GHz transition detected by Clancy et al. (2004), appear in the 1100–1260 GHz range. Fig. 6 shows a couple of lines around 1159 GHz. For a mean mixing ratio of 10^{-7}, the strongest transition, at 1159.8 GHz, shows a depth of 20%. The detection of H_2O_2 with HIFI should be possible with HIFI for any mixing ratio higher than 10^{-8} (i.e. any column density above 2×10^{15} cm^{-2}), and maps of H_2O_2 over the martian disk should be available in the future with ALMA.

4.6. HO_2 radical

HO_2 is a crucial intermediate species in photochemical models. The self recombination of HO_2, for example, is the main mechanism for the formation of H_2O_2. However, the photochemically predicted abundance of HO_2 is lower than the H_2O_2 abundance by at least an order of magnitude. In the submillimeter range, the intensities of the strongest HO_2 transitions occurring in the 1100–1260 GHz range are lower than the strongest H_2O_2 ones by a factor of about 4 (Table 3). We thus conclude that, if the photochemical models are correct, the detection of HO_2 with HIFI is probably unlikely.

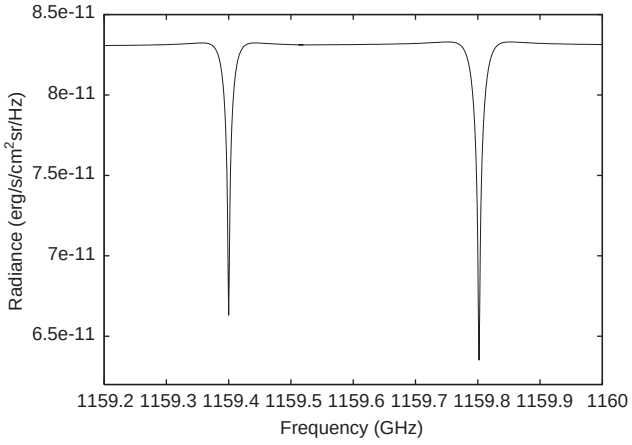

Fig. 6. Synthetic spectrum of the H_2O_2 absorption lines in the 1159.2–1160.0 GHz range, calculated for the integrated disk (HIFI simulation). The mean mixing ratio is $10^{-7}(2 \times 10^{17}$ $cm^{-2})$. The spectral resolution is 1 MHz ($R = 10^6$).

4.7. Nitrogen monoxide (NO)

NO was detected in the upper atmosphere of Mars by the Viking mass spectrometers (Nier and McElroy, 1977). In our previous analysis (Encrenaz et al., 1995), we concluded that NO could possibly be detected using a large ground-based submillimeter antenna at 651 GHz. However, the vertical distribution of NO which we used in those calculations was very optimistic, as it extrapolated the high-altitude measurements down to the troposphere. A more realistic model assumes that NO is entirely produced by photochemistry (Yung et al., 1977; McElroy et al., 1977), with no source coming from the surface. In 1999, a tentative detection of NO at 251 GHz using the IRAM 30 m antenna was announced (Encrenaz et al., 1999), but this observation was never confirmed, and the "detection" could have been some instrumental effect.

Assuming the vertical distribution derived from photochemical models, the expected NO column density is less than 10^{13} cm^{-2}. In view of the mean line intensities in the submillimeter range, the detection of NO with HIFI is most unlikely.

4.8. NO_2 and N_2O radicals

The NO_2 mixing ratio in Mars, according to photochemical models, is expected to be 100 times lower than the NO mixing ratio (Krasnopolsky, 1986). There is no information about N_2O, but its abundance is expected to be even lower. In view of the strengths of the millimeter transitions of both species, which are comparable to or lower than the NO ones, we can conclude that there detection on Mars with HIFI/Herschel is most unlikely.

4.9. Sulfur dioxide (SO_2)

In contrast with Venus, where an active sulfur chemistry takes place, no sulfur species have ever been detected in the atmosphere of Mars. We now consider the possibility of detecting sulfur species from possible local vents. Sulfur dioxide is one of the main components of vents on the Earth. Its present upper limit (3×10^{-8}) was first derived from millimeter ground-based observations of Mars (Encrenaz et al., 1991).

In the infrared range, several strong bands of SO_2 appear around 1300–1400 cm^{-1}, with a strong band head at 1361 cm^{-1}. Fig. 7 shows a synthetic spectrum of the absorption band for a mixing ratio of 10^{-7} and a spectral resolution of 0.1 cm^{-1}. At the band head around

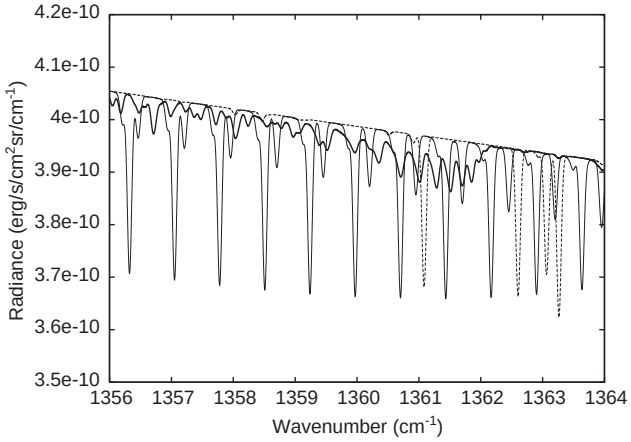

Fig. 7. Synthetic spectrum of the SO_2 absorption lines in the 1356–1364 cm^{-1} range. The mean mixing ratio is $10^{-7}(2 \times 10^{17}\,cm^{-2})$. The spectral resolution is 0.1 cm^{-1} ($R = 1.4 \times 10^4$). Bold solid line: SO_2 lines; thin solid lines: CO_2 thin dashed lines: H_2O lines.

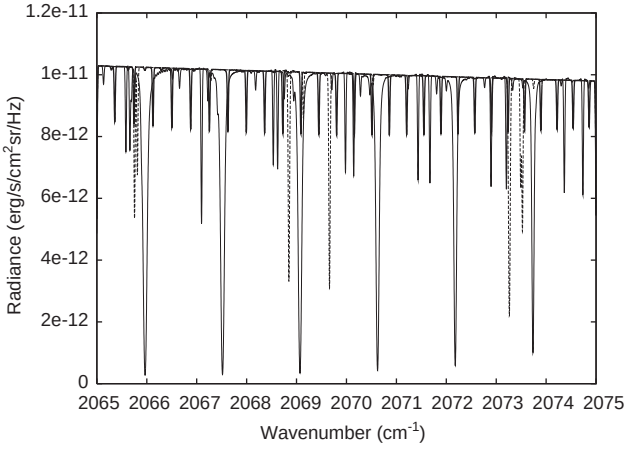

Fig. 8. Synthetic spectrum of OCS at 2066–2074 cm^{-1}(4.83 μm). The mean mixing ratio is $10^{-7}(2 \times 10^{17}\,cm^{-2})$. The spectral resolution is 0.03 cm^{-1} ($R = 7 \times 10^4$). Bold solid line: OCS lines; thin solid line: CO lines; thin dashed line: CO_2 lines.

1361 cm^{-1}, the expected depth is 2%. The molecule could be possibly detected from the ground with a high resolution spectrograph, like TEXES at IRTF.

In the case of submillimeter spectroscopy, there is little advantage in using high frequencies as compared to ground-based observations at 682 GHz using a large single dish. Sensitivity limits should be comparable, and longer integration times are expected to be available on ground-based facilities. As shown by Encrenaz et al. (1995), the detectability limit in this case is in the range of 10^{-9}. Lower limits are expected to be reached in the future with the ALMA interferometer.

4.10. Hydrogen sulfide (H_2S)

H_2S is another species possibly outgassed by local vents. Its present upper limit, obtained over the integrated disk from millimeter spectroscopy, is 3×10^{-8} (Encrenaz et al., 1991).

H_2S vibration–rotation bands in the infrared range are weak. The only hope to improve the H_2S upper limit is to use the submillimeter region. As in the case of SO_2, using a large-dish antenna is the best way to achieve a sensitive upper limit. A detectability limit of 10^{-9} could be achieved at 611 GHz using a 10 m size antenna (Encrenaz et al., 1995). As in the case of SO_2, improved limits, and spatially resolved measurements, could be obtained in the future with ALMA.

4.11. Carbonyl sulfide (OCS)

The upper limit of OCS on Mars, as derived from IRIS-Mariner 9 measurements, is 10^{-8} (Maguire, 1977). A strong band occurs around 2070 cm^{-1}(4.83 μm) and could be used with PFS or ground-based high-resolution measurements (CRIRES). Fig. 8 shows the synthetic spectrum of OCS around 2070 cm^{-1}, with a spectral resolution of 0.03 cm^{-1}. The corresponding depth of the individual lines is 20%. Reaching an upper limit of about 3×10^{-9} should thus be achievable with an instrument like CRIRES. OCS cannot be detected at the moderate spectral resolution of PFS because all individual lines contribute to a featureless continuum. In the millimeter/submillimeter range, OCS transitions are strongest around 400 GHz. OCS should be searched for using a large ground-based single-dish antenna; the expected detectability limit is in the range of 10^{-9} (Encrenaz et al., 1995).

4.12. SO and CS radicals

SO and CS are photochemical products of SO_2, H_2S, and OCS. Similar to their parent molecules, SO and CS exhibit submillimeter transitions in the 600–700 GHz range, observable from the ground, which are best suited for a study with a ground-based single-dish antenna. We thus adopt in the present study the detectability limits derived in our previous analysis (Encrenaz et al., 1995).

4.13. Formaldehyde (CH_2O)

The presence of formaldehyde was expected from some photochemical models (Moreau et al., 1992). Only hot spot models predict CH_2O, but at parts per trillion levels, and its tentative detection with Auguste-PHOBOS was reported with a mixing ratio of 5×10^{-7} (Korablev et al., 1993).

In the infrared range, the best spectral range to search for CH_2O is around 2820 cm^{-1}. Fig. 9 shows the synthetic spectrum of Mars for a mixing ratio of 10^{-7} and a spectral resolution of 0.03 cm^{-1}. The depths of the

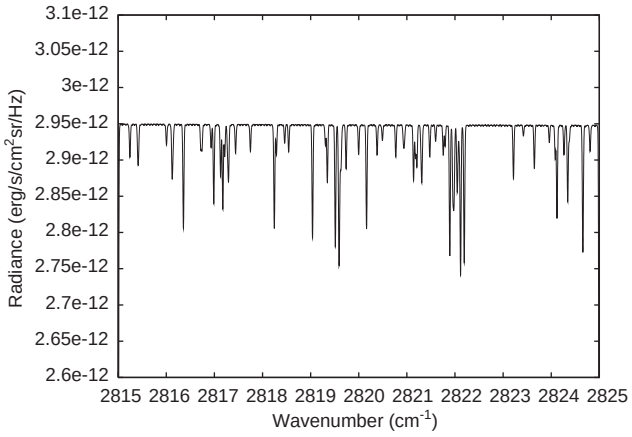

Fig. 9. Synthetic spectrum of H_2CO at 2816–2824 cm^{-1}(4.83 μm). The mean mixing ratio is 10^{-7}(2×10^{17} cm^{-2}). The spectral resolution is 0.03 cm^{-1}($R = 7 \times 10^4$).

strong lines are about 7%. Using a instrument like CRIRES and aiming at a S/N of 100 in the continuum in 1 h, a detection limit of 3×10^{-9}, as obtained by Krasnopolsky et al. (1997), is reachable in a few hours.

In the millimeter/submillimeter range, the strongest CH_2O transitions occur between 600 and 1300 GHz. As in the case of SO_2 and H_2S, single-dish antenna working above 600 GHz will be best suited to search for CH_2O. The expected detection limit is 10^{-10} (Encrenaz et al., 1995).

4.14. Methane (CH_4)

Methane has been tentatively detected on Mars during the 2003 opposition, from ground-based nfrared high-resolution spectroscopy (Mumma et al., 2003; Krasnopolsky et al., 2004), and from PFS/Mex (Formisano et al., 2004a) at a level of about 10 ppb. According to the authors, CH_4, which should be destroyed by photochemical processes in a few hundred years, probably originates from outgassing.

In the infrared range, the strongest methane bands appear at 3.3 μm (ν_3) and 7.7 μm (ν_4). The near-infrared band is more suitable for detection, because it is intrinsically stronger, and appears in the reflected component (more favorable for enhancing contrasts). In addition, in the case of PFS, the NEB is almost ten time more favorable below 5 μm.

An estimate of the CH_4 detection limit achievable with the PFS can be obtained by using the ISO spectrum (Lellouch et al., 2000). As shown in the Fig. 7 of this paper, an upper limit of 5×10^{-8} is derived, corresponding to a band depth of 1.5%. The continuum level is about 0.25 erg/s/cm^2 sr/cm^{-1}. Assuming a NEB of 0.05 erg/s/cm^2 sr/cm^{-1}, the expected S/N in 1 s is 5. A S/N of 300, required to reach the upper limit of 5×10^{-8}, should be achievable in 1 h of integration time. It can be seen that PFS is well suited for studying CH_4 using long integration times. If strong CH_4 outgassing takes place from local hot spots on Mars, PFS could also detect it at the level of 400 ppb in 1 min integration time.

4.15. Ammonia (NH_3)

A stringent upper limit (5×10^{-9}) was obtained for ammonia with the IRIS-Mariner 9 observations at 10.5 μm (Maguire, 1977). A better upper limit is likely to be obtained with PFS observations integrated over many orbits, as the spectral resolution of PFS is twice better. This instrument is also well suited for searching for NH_3 in hot spots, if ammonia is present in larger abundances.

Another upper limit can be obtained from rotational lines in the submillimeter range. Fig. 10 shows a synthetic spectrum of NH_3 at 1214.9 GHz, using a NH_3 mixing ratio of 5×10^{-9}. The expected depth is about 10%, both for disk-integrated and disk-resolved observations. As mentioned above, we expect a S/N of 100 in the continuum in about 70 s. An NH_3 mixing ratio of 5×10^{-9} could thus be detectable, under best conditions, in about 1 min of integration time.

4.16. Phosphine (PH_3)

There is no indication about the possible presence of PH_3 on Mars. However, this species has been detected in the atmospheres of Jupiter and Saturn (e.g. Atreya et al., 2003 review), and could also be a component of the material outgassed from any hot spots on Mars. An upper limit of 10^{-7} was obtained for PH_3 from IRIS-Mariner 9 (Maguire, 1977). We can expect, over the whole martian disk, a comparable upper limit from PFS,

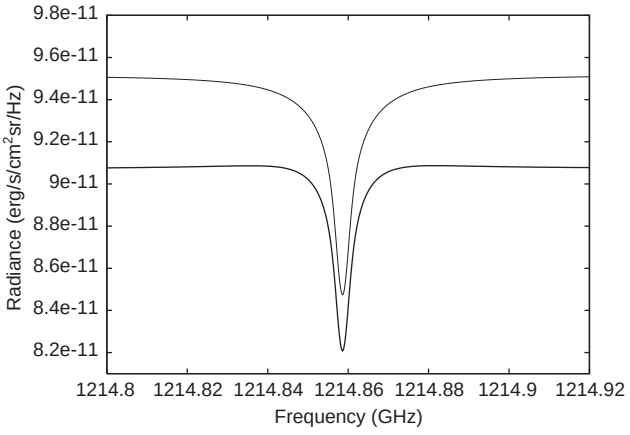

Fig. 10. Synthetic spectrum of NH_3 near 1214.9 GHz, assuming disk-integrated observations (bold line, HIFI simulation) and an airmass of 1.6 (thin line, ALMA simulation). The mean mixing ratio is 5×10^{-9}. The spectral resolution is 1 MHz ($R = 10^6$).

whose spectral resolution is twice better than that of IRIS.

In the submillimeter range, PH_3 exhibits a series of strong rotational transitions. For a PH_3 mixing ratio of 10^{-7}, the expected line depth of the strongest line, around 1167 cm^{-1}, is about 13%, both for disk-integrated and disk-resolved calculations. An upper limit of 10^{-8} could thus be reached in about one minute integration time. However we must remember that PH_3 is not likely to be uniformly distributed over the disk, but, if present, will rather be outgassed from local sources.

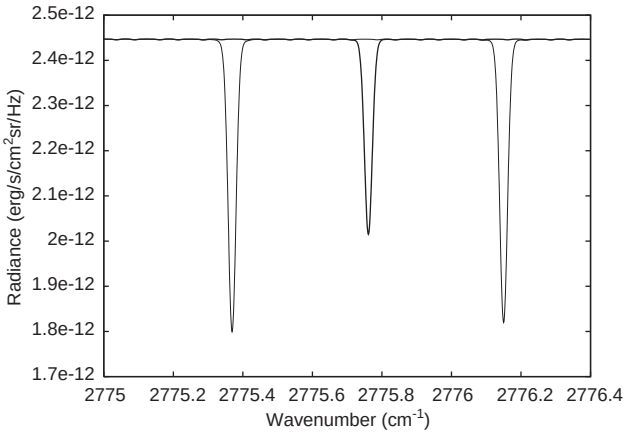

Fig. 11. Synthetic spectrum of HCl near 2775.8 cm^{-1}. The mean mixing ratio is 10^{-7}. The spectral resolution is 0.03 cm^{-1} ($R = 10^5$). Solid line: HCl line; dashed line: CO_2 lines.

4.17. Hydrogen chloride (HCl)

There is presently no information about the HCl abundance on Mars. However, HCl could be outgassed from hotspots, as on Earth, but in very small amounts (Wong et al., 2003). HCl has been detected on Venus with a mixing ratio of 4×10^{-7}, from ground-based high-resolution spectroscopy in the near-infrared (Connes et al., 1967). A stringent upper limit of 2×10^{-9} was obtained from high-resolution ground-based observations of Mars (Krasnopolsky et al., 1997).

Fig. 11 shows the synthetic spectrum of HCl in the near-IR range at 3.6 μm, assuming a mixing ratio of 10^{-7}, with a spectral resolution of 0.03 cm^{-1} ($R = 10^5$). This high resolution will be achievable with the CRIRES instrument. The expected depth of the line is close to 20%. Using CRIRES, we should be able to get an HCl detection limit of about 2×10^{-9}, with adequate spatial resolution. With the 2 cm^{-1} resolution of the PFS, the detectability limit of HCl is strongly degraded. Assuming, as for CH_4, a S/N of 5 in 1 s integration time in the continuum, we can hope to get a S/N of 8 for HCl in a 20% depth line in about 1 min. We should be able to reach an upper limit of 10^{-6} in about 1 min.

HCl also exhibits strong rotational lines in the submillimeter range. Fig. 12 shows the HCl spectrum of the integrated disk around 1251.5 GHz, for an HCl mixing ratio of 5×10^{-9}. The corresponding line depth is 20%. We can thus hope to reach an upper limit of 3×10^{-10} in about 1 min integration time.

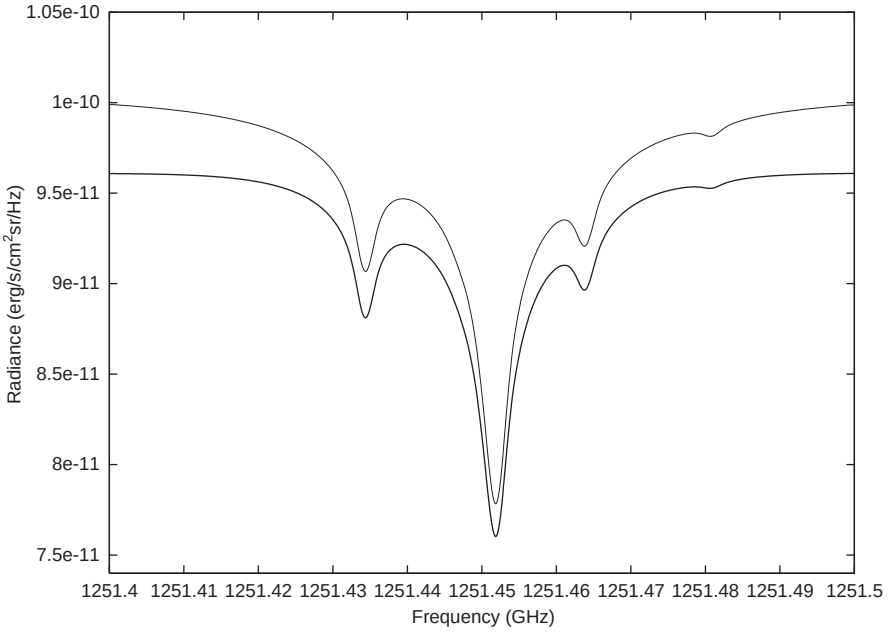

Fig. 12. Synthetic spectrum of HCl near 1251.5 GHz, , assuming disk-integrated observations (bold line, HIFI simulation) and an airmass of 1.6 (thin line, ALMA simulation). The mean mixing ratio is 5×10^{-9}. The spectral resolution is 1 MHz ($R = 10^6$).

5. Conclusions

(1) The PFS will be best suited for mapping H_2O and CO, monitoring the water cycle, and investigating possible local variations of CO. HDO is expected to be detectable when the water vapor abundance is close to its maximum value. A more precise determination of the D/H ratio is also expected. Other minor species could possibly be detected. In particular, the CH_4 abundance could be confirmed at 3.3 μm. For other minor species, upper limits comparable to the ones derived by IRIS/Mariner 9 (Maguire, 1977) can be expected. We note that the upper limits derived by Maguire et al. (1977) were obtained from an integration of all data, which corresponded to an effective NEB of $0.012\,erg/s/cm^2\,sr/cm^{-1}$ while in the case of PFS, the NEB is $0.4\,erg/s/cm^2\,sr/cm^{-1}$ per spectrum (with an integration time of 10 s per spectrum). We can thus expect to obtain upper limits comparable to Maguire's values in an integration time of a few hours.

(2) HIFI will provide the best measurements of H_2O and its isotopes. In particular, HIFI is expected to yield the most accurate results on the D/H, $^{16}O/^{18}O$ and $^{16}O/^{17}O$ ratios in the atmosphere of Mars. HIFI should be able to detect O_2 and H_2O_2 in 1 min integration time, and O_3 in a few hours integration time.

(3) HIFI may also improve the globally averaged detection limits for some minor species. The most favorable spectral range is in the 1100–1260 GHz interval which corresponds to the best receiver sensitivity. Among the species which could be detected in this spectral range are O_2, H_2O_2 and possibly O_3, while stringent upper limits could be obtained for HCl, NH_3 and PH_3.

(4) The sulfur species (SO_2, H_2S, OCS) have rotational transitions whose intensities in the submillimeter frequency range of 400–700 GHz are only slightly lower than in the 1100–1260 GHz range. In addition, many of these transitions are observable from the ground. In this case, large ground-based single-dish antennas, which could benefit from longer exposure times, are expected to provide the most sensitive upper limits. The same conclusion holds for CH_2O, as well as SO and CS (Encrenaz et al., 1995). In the future, ALMA will be best

Table 4
Summary of expected detectabilities

Species	Detectability IR (PFS)	Detectability IR (ground-based)	Detectability sub-mm (HIFI/GB)	Comment
(16)CH_4	3×10^{-8}	Detected	—	To be searched for with PFS
(17)NH_3	5×10^{-9}	About 5×10^{-10}	5×10^{-10}	To be searched for with PFS
(18)H_2O	Detectable	Detected	Detected(SWAS)	Water cycle mon.
(19)HDO	Detectable	Detected	Detected (SWAS)	D/H(PFS + HIFI)
(19)$H_2^{17}O$	—	—	Detected (SWAS)	^{17}O ^{16}O(HIFI)
(20)$H_2^{18}O$	—	—	Detected (SWAS)	$^{18}O^{16}O$(HIFI)
(28) CO	Detectable	Detected	Detected (GB)	PFS:Search for local variations $^{13}C/^{12}C$ (HIFI/ALMA)
(29)^{13}CO	Detectable	Detected	Detected (GB)	
(29)$C^{17}O$	—	—	—	
(30)$C^{18}O$	—	Detectable	Detectable	$^{18}O/^{16}O$ (CRIRES, HIFI, ALMA)
(30)CH_2O	3×10^{-8}[a]	3×10^{-9}	10^{-10}	CSO/HIFI/ALMA[b]
(30)NO	—	—	—	Detection unlikely
(32)O_2	—	—	Detectable	Possible Detection (HIFI)
(33)HO_2	—	—	—	Detection unexpected
(34)H_2S	—	—	10^{-9}	CSO/HIFI/ALMA[b]
(34)H_2O_2	—	Detected	Detected	Ground-based observations favorable for detection
(34)PH_3	10^{-7}	About 10^{-8}	10^{-8}	To be searched for with PFS
(35) HCl	1.5×10^{-8}	2×10^{-9}	3×10^{-10}	To be searched for with PFS
(44)CS	—	—	10^{-10}	CSO/HIFI/ALMA[b]
(48)O_3	—	Detected	—	Best observed from GB-HR spectroscopy
(48)SO	—	—	10^{-10}	CSO/HIFI/ALMA[b]
(60)OCS	7×10^{-8}[a]	6×10^{-9}	10^{-9}	CSO/HIFI/ALMA[b]
(64)SO_2	3×10^{-8}[a]	5×10^{-8}	10^{-9}	CSO/HIFI/ALMA[b]

[a]From Maguire (1977).
[b]From Encrenaz et al. (1995).

suited for searching undetected minor species at high spatial resolution such as SO_2, SO, H_2S, OCS, CH_2O, PH_3, and HCl, all of which have transitions observable from the ground.

(5) Ground-based high-resolution spectrometers such as CRIRES on the VLT should be able to place better upper limits or detect several species, including CH_2O at 3.55 μm, and HCl at 3.60 μm.

(6) The 7–13 μm region which is accessible from the ground is especially suitable for mapping H_2O_2 (at 8.1 μm), for searching for SO_2 (at 7–8 μm), and for mapping O_3 (at 9–10 μm) when the planetary Doppler shift is maximum (Table 4).

Acknowledgements

We thank P. Hartog for his calculations of the expected sensitivity limits of HIFI. TE acknowledges support from the Centre National de la Recherche Scientifique. SKA acknowledges support from NASA's Mars Program Office at JPL for his participation on the Mars Express Project.

References

Atreya, S.K., Gu, Z., 1994. Stability of the martian atmosphere: Is heterogeneous catalysis essential? J. Geophys. Res. 99, 13133–13145.

Atreya, S.K., Mahaffy, P.R., Niemann, H.B., Wong, M.H., Owen, T.C., 2003. Composition and origin of the atmosphere—an update and implications for the extrasolar giant planets. Planet. Space Sci. 51, 105–112.

Billebaud, F., Maillard, J.-P., Lellouch, E., Encrenaz, T., 1992. The spectrum of Mars in the (1-0) vibrational band of CO. Astron. Astrophys. 261, 647–657.

Billebaud, F., Rosenqvist, J., Lellouch, E., Maillard, J.-P., Encrenaz, T., Hourdin, F., 1998. Observations of CO in the atmosphere of Mars in the (2-0) vibrational band at 2.35 μm. Astron. Astrophys. 333, 1092–1099.

Biver, N., Lecacheux, A., Crovisier, J. et al., 2004. Observations of $H_2O, H_2{}^{18}O$ and CO in Mars with Odin. Communication presented at the COSPAR General Assembly, Paris, July 2004.

Carleton, N.P., Traub, W.A., 1972. Detection of molecular oxygen on Mars. Science 177, 988–992.

Clancy, R.T., Muhleman, D.O., Berge, G.L., 1990. Global changes in the 0–70 km thermal structure of Mars atmosphere derived from 1975–1989 microwave CO spectra. J. Geophys. Res. 95, 14543–14554.

Clancy, R.T., Grossman, A.W., Muhleman, D.O., 1992. Mapping Mars water vapor with the Very Large Array. Icarus 122, 36–62.

Clancy, R.T., et al., 1996. Water vapor saturation at low altitudes around Mars aphelion: a key to martian climate? Icarus 122, 36–62.

Clancy, R.T., Sandor, B.J., Moriarty-Schieven, G.H., 2004. A measurement of the 362 GHz absorption line of Mars atmospheric H_2O_2. Icarus 168, 116–121.

Connes, P., Connes, J., Benedict, W.J., Kaplan, L.D., 1967. Traces of HCl and HF in the atmosphere of Venus. Astrophys. J. 147, 1230–1237.

Encrenaz, Th., 2001. The atmosphere of Mars as constrained by remote sensing. Space Sci. Rev. 96, 411–424.

Encrenaz, Th., et al., 1991. The atmospheric composition of Mars: ISM and ground-based observational data. Annales Geophys. 9, 797–803.

Encrenaz, Th., et al., 1995. Detectability of molecular species in planetary and satellite atmospheres from their rotational transitions. Planet. Space Sci. 43, 1485–1516.

Encrenaz, Th., Lellouch, E., Paubert, G., Gulkis, S., 1999. IAUC 7186, June 4.

Encrenaz, Th., Lellouch, E., Paubert, G., Gulkis, S., 2001a. The water vapor vertical distribution on Mars from millimeter transitions of HDO and $H_2{}^{18}O$. Planet. Space Sci. 49, 731–741.

Encrenaz, Th., et al., 2001b. The Mars flyby of Rosetta: an opportunity for infrared and microwave high-resolution sounding. Planet. Space Sci. 49, 673–687.

Encrenaz, Th., et al., 2002. A stringent upper limit of the H_2O_2 abundance in the martian atmosphere. Astron. Astrophys. 396, 1037–1044.

Encrenaz, T., Bézard, B., Greathouse, T.K., Lacy, J.H., Richter, M.J., Atreya, S.K., Wong, A.S., 2003. Mars. IAU Circ. 8254.

Encrenaz, T., Bézard, B., Greathouse, T.K., Lacy, J.H., Richter, M.J., Atreya, S.K., Wong, A.S.,2004. Hydrogen peroxide on Mars: evidence for spatial and temporal variations. Icarus 170, 424–429.

Espenak, F., Mumma, M.J., Kostiuk, T., 1991. Ground-based infrared measurements of the global distribution of ozone in the atmosphere of Mars. Icarus 92, 252–262.

Formisano, V., Atreya, S.K., Encrenaz, T., Ignatiev, N., Giuranna, M., 2004a. In preparation.

Formisano V., Atreya, S.K., Encrenaz, T., Ignatiev, N., Giuranna, M., 2004b. First results of the Planetary Fourier Spectrometer aboard Mars Express. Icarus, submitted for publication.

Gurwell, M., et al., 2000. Submillimeter Wave Astonomical Satellite observations of the martian atmosphere: temperature and vertical distribution of water vapor. Astrophys. J. 539, L151–L154.

Jacquinet-Husson, N., et al., 1999. The 1997 spectroscopic GEISA databank. J. Quant. Spectrosc. Radiat. Transfer 62, 205–254.

Jakosky, B., Haberle, R., 1992. The seasonal behavior of water on Mars. In: Kieffer, H.H, et al. (Ed.), Mars. University of Arizona Press, pp. 969–1016.

Kakar, R.K., Water, J.W., Wilson, W.J., 1977. Mars: microwave detection of carbon monoxide. Science 196, 1090–1091.

Klein, H.P., Horowitz, N.H., Biemann, K., 1992. The search for extant life on Mars. In: Kieffer, H.H., et al. (Ed.), Mars. University of Arizona Press, pp. 1221–1233.

Korablev, O.I., et al., 1993. Tentative detection of formaldehyde in the martian atmosphere. Planet. Space Sci. 41, 441–451.

Krasnopolsky, V.A., 1986. Photochemistry of the atmospheres of Mars and Venus. Springer, Berlin.

Krasnopolsky, V., 1993. Photochemistry of the martian atmosphere (Mean Conditions). Icarus 101, 313–332.

Krasnopolsky, V.A., 2003. Spectroscopic mapping of Mars CO mixing ratio: detection of north-south asymmetry. J. Geophys. Res. 108, E2, doi:10.1029/2002/JE001926.

Krasnopolsky, V.A., Bjoraker, G.J., Mumma, M.J., Jennings, D.E., 1997. High-resolution spectroscopy of Mars at 3.7 and 8 μm: a sensitive search for H_2O_2, H_2CO, HCl and detection of HDO. J. Geophys. Res. 102, 6525–6534.

Krasnopolsky, V.A., Maillard, J.-P., Owen, T.C., 2004. Detection of methane in the martian atmosphere: evidence for life. Communication presented at the EGU Assembly, Nice, April 2004.

Lellouch, E., Gerin, M., Combes, F., Atreya, S.K., Encrenaz, Th., 1989. Observations of the $J = 1$-0 CO lines in the Mars atmosphere: radiodetection of ^{13}CO and monitoring of ^{12}CO. Icarus 77, 414–438.

Lellouch, E., Rosenqvist, J., Goldstein, J.J., Bougher, S.W., Paubert, G., 1991. First absolute wind measurements in the middle atmosphere of Mars. Astrophys. J. 383, 401–406.

Lellouch, E., et al., 2000. The 2.4 – 45 μm spectrum of Mars observed with the Infrared Space Observatory. Planet. Space Sci. 48, 1393–1405.

McElroy, M.B., Kong, T.Y., Yung, Y.L., 1977. Photochemistry and evolution of Mars' atmosphere: a Viking perspective. J. Geophys. Res. 82, 4379–4388.

Maguire, W.C., 1977. Martian isotopic ratios and upper limits for possible minor constituents as derived from Mariner 9 infrared spectrometer data. Icarus 32, 85–97.

Martin, T.Z., Kieffer, H.H., 1979. Thermal infrared properties of the martian atmosphere. 2. The 15 μm band measurements. J. Geophys. Res. 84, 2843–2852.

Moreau, D., Falise, E., Muller, C., Rosenqvist, R., Marten, A., Korablev, O., Esposito, L.W., 1992. Organic chemistry in the current Martian atmosphere: theoretical and experimental investigations. Bull. Amer. Astron. Soc. 24, 1015–1015.

Mumma, M.J., Novak, R.E., DiSanti, M.A., Bonev, B.P., 2003. A sensitive search for methane on Mars. Bull. Amer. Astron. Soc. 35, 937–938.

Nair, H., Allen, M., Anbar, A.D., Yung, Y.L., Clancy, R.T., 1994. A photochemical model of the martian atmosphere. Icarus. 111, 124–150.

Nier, A.O., McElroy, M.B., 1977. Composition and structure of Mars' upper atmosphere: results from the neutral mass spectrometers of Viking 1 and 2. J. Geophys. Res. 82, 4341–4349.

Novak, R.E., Mumma, M.J., DiSanti, M.A., Russo, N.D., Magee-Sauer, K., 2002. Mapping of Ozone and water in the atmosphere of Mars near the 1997. Aphelion. Icarus 158, 14–23.

Owen, T., et al., 1992. The composition and early history of the atmosphere of Mars. In: Kieffer, H.H (Ed.), Mars. University of Arizona Press, pp. 818–834.

Owen, T., Biemann, K., Biller, J.E., Lafleur, A.L., Rushneck, D.R., Howarth, D.W., 1977. The composition of the atmosphere at the surface of Mars. J. Geophys. Res. 82, 4635–4639.

Owen, T., Maillard, J.-P., de Bergh, C., Lurz, B.L., 1988. Deuterium on Mars: the abundance of HDO and the value of D/H. Science 240, 1767–1770.

Perrin, A., Flaud, J.-M., Camy-Peyret, C., Schermaul, R., Winnewisser, M., Mandin, J.-Y., Dana, V., Badaoui, M., Koput, J., 1996. J Mol. Spectroc. 176, 287–296.

Rosenqvist, J., Drossart, P., Combes, M., Encrenaz, T., Lellouch, E., Bibring, J.-P, Erard, S., Langevin, Y., Chassefiere, E., 1992. Minor constituents in the Martian atmosphere from the ISM/Phobos experiment. Icarus 98, 254–270.

Santee, M., Crisp, D., 1993. Thermal structure and dust loading of the martian atmosphere during last southern summer: Mariner 9 revisited. J. Geophys. Res. 98, 3261–3279.

Smith, M.D., 2002. The annual cycle of water vapor on Mars as observed by the Thermal Emission Spectrometer. J. Geophys. Res. 107 (E11), 1–25.

Smith, M.D., Pearl, J.C., Conrath, B.J., Christensen, P.R., 2001. One Martian year of atmospheric observations with the Thermal Emission Spectrometer. J. Geophys. Res. Lett. 28, 4263–4266.

Wong, A.S., Atreya, S.K., Encrenaz, Th., 2003. Chemical markers of possible hot spots on Mars. J. Geophys. Res. 108 (E4), 1–7.

Yung, Y.L., Strobel, D.F., Kong, T.Y., McElroy, M.B., 1977. Photochemistry of nitrogen in the martian atmosphere. Icarus 30, 26–41.